2014 RISP International Workshop on Nonlinear Circuits,
Communications and Signal Processing
NCSP'14, Honolulu, Hawaii, USA. February 28 - March 3, 2014

Chaotic Circuit Generating Two Main Frequency Band Oscillations

Yasuteru Hosokawa[1] and Yoshifumi Nishio[2]

[1] Shikoku University
Furukawa, Ohjin, Tokushima, Japan
Phone:+81-88-665-1300
FAX:+81-88-637-1318
E-mail: hosokawa@keiei.shikoku-u.ac.jp

[2] Tokushima University
2-1 Minami-Josanjima, Tokushima, Japan
Phone:+81-88-656-7470
FAX:+81-88-656-7471
E-mail: nishio@ee.tokushima-u.ac.jp

abstract

In this study, novel chaotic circuit generating two main frequency band oscillations is proposed. We consider that this circuit is suitable for finding a novel phenomena related to quasi-synchronization.

1. Introduction

Many kinds of interesting phenomena have been observed in coupled chaotic circuits. One topic of coupled chaotic circuits is a chaotic synchronization. A chaotic synchronization is a phenomenon that orbits of coupled chaotic oscillators become same. There are many studies about a chaotic synchronization. Especially, we pay attention to a chaotic quadi-synchronization. In large-scale coupled chaotic circuits, chaotic quadi-synchronization is observed and some related phenomena are observed. The observed phenomena are influenced by a coupling strength, a topology of the system and characteristics of coupled circuits. The coupling strength and the topology can be changed easily. However, changing the characteristics of coupled circuits is not easily, because of there are not so much the number of chaotic circuits. In order to progress the study of coupled chaotic circuit systems, many kinds of chaotic circuits are needed.

In this study, novel chaotic circuit generating two main frequency band oscillations is proposed. Normally, a chaotic oscillation has a continuous frequency band including main frequency. We consider that this circuit is suitable for finding a novel phenomena related to quasi-synchronization.

2. Proposed circuit

Figure 1 is a proposed circuit in this study. The circuit consists of two capacitors, two inductors, two diodes and one negative resistor. By two L-C set, two main bands are generated. Parameters C_1 and L_1 are set as smaller values than parameters C_2 and L_2.

In order to derive a circuit equation, bidirectionally coupled diodes are modeled as a piecewise linear function shown in Fig. 2. By using this model, the circuit equation is described as follows:

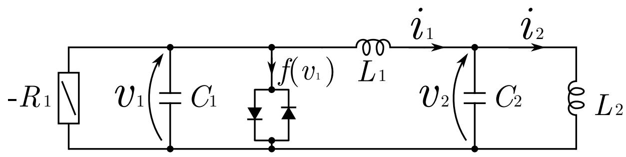

Figure 1: Proposed circuit.

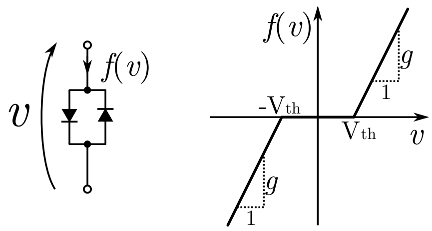

Figure 2: Bidirectionally coupled diode model.

$$\begin{cases} C_1 \dfrac{dv_1}{dt} = \dfrac{1}{R_1} v_1 - i_1 - f(v_1), \\ L_1 \dfrac{di_2}{dt} = v_1 - v_2, \\ C_2 \dfrac{dv_3}{dt} = i_1 - i_2, \\ L_2 \dfrac{di_4}{dt} = v_2, \end{cases} \tag{1}$$

where

$$f(v) = gv_1 + g(|v_1 - V_{th}| - |v_1 + V_{th}|)/2. \tag{2}$$

By substituting the variables and the parameters,

$$\begin{aligned}
&x_1 = \frac{v_1}{V_{th}}, \quad x_2 = \sqrt{\frac{L_1}{C_1}}\frac{i_1}{V_{th}}, \quad x_3 = \frac{v_2}{V_{th}}, \\
&x_4 = \sqrt{\frac{L_1}{C_1}}\frac{i_2}{V_{th}}, \quad \frac{d}{dt} = \text{" $\cdot$ "}, \quad \tau = \frac{1}{\sqrt{L_1 C_1}}t, \\
&\alpha = \frac{1}{R_1}\sqrt{\frac{L_1}{C_1}}, \quad \beta = \frac{C_1}{C_2}, \quad \gamma = \frac{L_1}{L_2} \text{ and } \delta = g\sqrt{\frac{L_1}{C_1}}.
\end{aligned} \tag{3}$$

equations (1) and (2) are normalized as

$$\begin{cases} \dot{x}_1 &= \alpha x_1 - x_2 - x_d, \\ \dot{x}_2 &= x_1 - x_3, \\ \dot{x}_3 &= \beta(x_2 - x_4), \\ \dot{x}_4 &= \gamma x_3, \end{cases} \tag{4}$$

where

$$x_d = \delta x_1 + \delta(|x_1 - 1| - |x_1 + 1|)/2. \tag{5}$$

3. Exact solutions and Poincaré Map

Since the circuit equations (4) are piecewise-linear, solutions in each linear region can be derived. At first, we define three piecewise-linear region as follows.

$$\begin{aligned} \mathbf{R_1}: &\quad x_1 > 1. \\ \mathbf{R_2}: &\quad -1 \le x_1 \le 1. \\ \mathbf{R_3}: &\quad x_1 < -1. \end{aligned} \tag{6}$$

The eigenvalues in each region are calculated from Eq. (4). The eigenvalues in each region are described as follows.

$$\begin{aligned} \mathbf{R_1} \text{ and } \mathbf{R_3}: &\quad \lambda_{11}, \ \lambda_{12}, \ \sigma_{11} \pm j\omega_{11}. \\ \mathbf{R_2}: &\quad \sigma_{21} \pm j\omega_{21}, \ \sigma_{22} \pm j\omega_{22}. \end{aligned} \tag{7}$$

The eigenvalues in each region are obtained from the 4th order eigenequation of Eq. (4). The equilibrium points of each region are calculated by putting the right side of Eq. (4) to be equal to zero. Then, the solutions in each linear region can be described. We omit the description, because it is complicated enough to write here.

Now, we are deriving the Poincaré map and the Jacobian matrix.

Let us define the following subspace

$$\mathbf{S} = \mathbf{S_1} \cap \mathbf{S_2}. \tag{8}$$

where,

$$\begin{aligned} \mathbf{S_1}: &\quad x_1 = 1, \\ \mathbf{S_2}: &\quad x_2 > \alpha. \end{aligned} \tag{9}$$

The subspace $\mathbf{S_1}$ corresponds to the boundary condition between $\mathbf{R_1}$ and $\mathbf{R_2}$, while the subspace $\mathbf{S_2}$ corresponding to the condition $\dot{x}_1 < 0$. Namely, $\mathbf{S}$ corresponds to the transitional condition from $\mathbf{R_1}$ to $\mathbf{R_2}$.

Let us consider the solution starting from an initial point on $\mathbf{S}$. The solution returns back to $\mathbf{S}$ again after wandering $\mathbf{R_1}$, $\mathbf{R_2}$ and $\mathbf{R_3}$. Hence, we can derive the Poincaré map as follows.

$$\mathbf{T}: \quad \mathbf{S} \to \mathbf{S}, \quad \mathbf{x_0} \mapsto \mathbf{T}(\mathbf{x_0}). \tag{10}$$

where, $\mathbf{x_0}$ is an initial point on $\mathbf{S}$, while $\mathbf{T}(\mathbf{x_0})$ is the point at which the solution starting from $\mathbf{x_0}$ hits $\mathbf{S}$ again. $\mathbf{T}(\mathbf{x_0})$ can be derived by using the exact solutions. The Jacobian matrix $\mathbf{DT}$ of the Poincaré Map $\mathbf{T}$ can be also derived.

We can calculate the largest Lyapunov exponent by

$$\mu = \lim_{N\to\infty} \frac{1}{N}\sum_{j=0}^{N} \log|\mathbf{DT}_j \cdot e_j|. \tag{11}$$

here e_j is a normalized base.

v_1

v_2

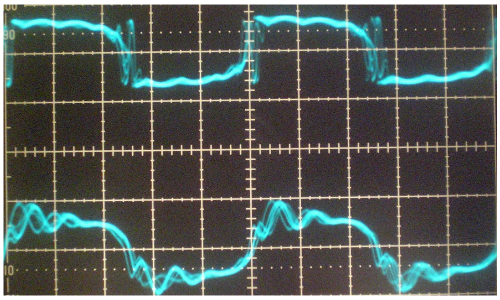

Figure 3: Waveform observed in the circuit experiment. $R_1 = 3.0[\mathrm{k}\Omega]$.

v_1

v_2

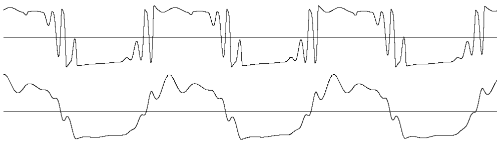

Figure 4: Waveform observed in the computer calculation. $\alpha = 0.6$.

4. Circuit Experiments And Computer Calculations

Figures 3, 4 and 5 are a circuit experiment results and a computer calculation results. In circuit experiments, circuit parameters are fixed as $C_1 = 0.015[\mu\mathrm{F}]$, $L_1 = 5[\mathrm{mH}]$, $C_2 = 0.10[\mu\mathrm{F}]$ and $L_2 = 100[\mathrm{mH}]$. Corresponding parameters of computer calculations are fixed as $\beta = 0.15$, $\gamma = 0.05$ and $\delta = 10$. Control parameters are set as R_1 and α.

Waveforms are shown in Figs 3 and 4. Long and short wavelengths are observed.

Projections of attractors onto v_1 and v_2 are shown in Fig. 5 (a). Projections of attractors onto x_1 and x_3 and their Poincaré maps are shown in Fig. 5 (b) and (c), respectively. Rows of Fig. 5 are corresponding to each others.

By changing control parameters, periodic orbits are observed in Figs. 5 (1), (2), (4) and (5). Chaotic phenomena are observed in Figs. 5 (3) and (6).

One-parameter bifurcation diagram and the calculated largest Lyapunov exponent are shown in Fig. 6 and Fig. 7, respectively. Bifurcation phenomena of periodic orbits, chaos, window and so on are observed. For $1.40 < \alpha < 7.80$, the largest Lyapunov exponent becomes positive though some large windows are observed. By using this result, We can say the generation of chaos is confirmed numerically. By changing other parameters, period doubling bifurcation phenomena, tours and so on are also observed in this circuit.

5. Conclusions

In this study, a novel chaotic circuit generating two main frequency band oscillations has been proposed. By circuit experiments, chaotic attractors have been observed and by using a linearized model, the generation of chaos has been confirmed numerically.

We consider that this circuit is suitable for finding a novel phenomena related to quasi-synchronization. Therefore, it is expected that this circuit contributes to studies of large scale coupled chaotic circuits.

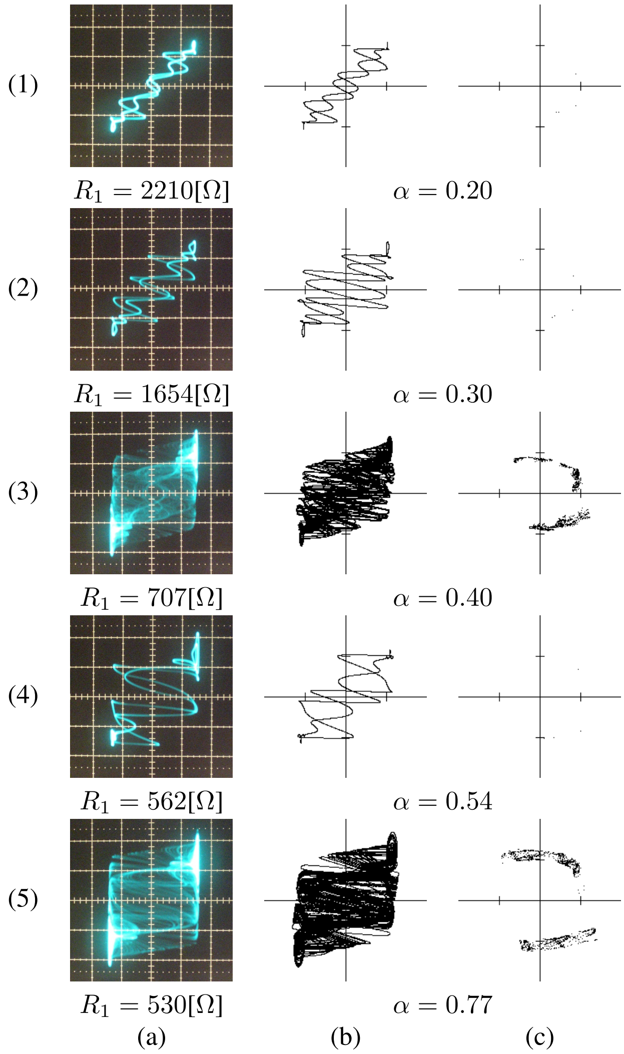

Figure 5: Circuit Experimental Results and Computer Calculation Results. (a) Circuit Experiments. v_1-v_2. (b) Attractors. x_1-x_2. (c) Poincaré maps. v_1-v_3.

References

[1] L. M. Pecora and T. L. Carrol, "Synchronization in Chaotic Systems," *Physical Review Letters*, vol. 64, pp. 821–824, 1990.

[2] T. Endo, and S. Mori, "Mode Analysis of a Ring of a Large Number of Mutually Coupled van der Pol Oscillators," *IEEE Trans. Circuit and Systems*, vol. CAS-25, no. 5, pp. 7–18, 1978.

[3] D. A. Linkens, "Analytical solution of large numbers of mutually-coupled nearly-sinusoidal oscillators," *IEEE Trans. Circuits and Systems*, vol. CAS-21, pp.294–300, Mar, 1974.

[4] H. Sekiya, S. Moro, S. Mori, and I. Sasase, "Synchronization Phenomena on Four Simple Chaotic Oscillators Full-Coupled by Capacitors," *IEICE Trans. Fundamentals*, vol. J82-A, No. 3, pp.375–385, 1999.

[5] M. Miyamura, Y. Nishio and A. Ushida, "Clustering in Globally Coupled System of Chaotic Circuits," *IEEE Proc. ISCAS'02*, vol. 3, pp. 57–60, 2002.

[6] Y. Hosokawa, R. Tsujioka and Y. Nishio, "Relation between Synchronous Rate and Small Variations on an Asymmetrical Coupled Chaotic System," *Proc. NOLTA'05*, pp. 166–169, 2005.

[7] Y. Hosokawa and Y. Nishio, "Asymmetrical Chaotic Coupled System Using Two Different Parameter Sets," *Proc. NOLTA'06*, pp. 543–546, Sep. 2006.

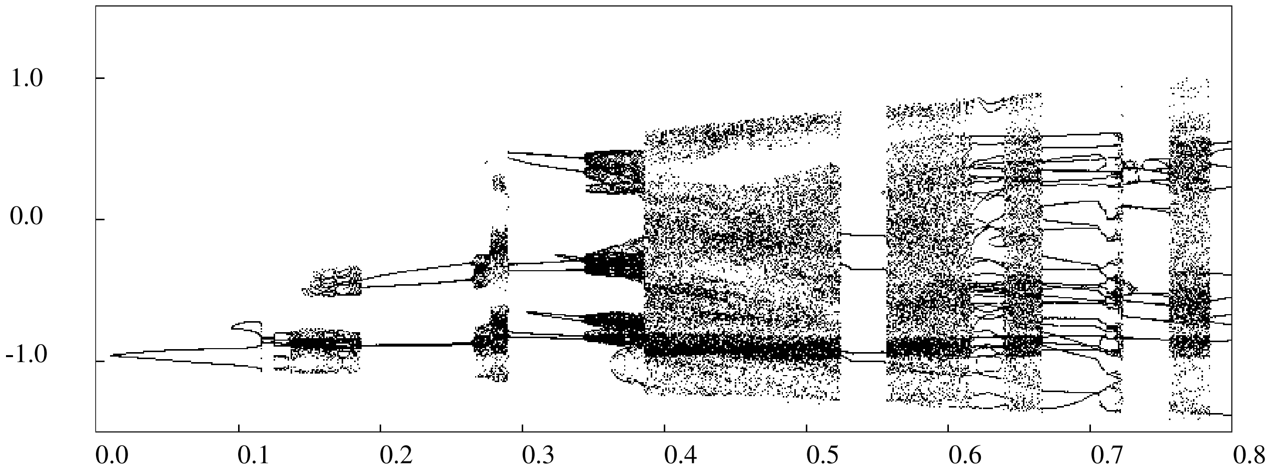

Figure 6: One parameter bifurcation diagram. Vartical axis: x_3. Horizontal axis: α. $0.01 \leq \alpha \leq 0.80$. Parameter Step: 0.001. Plotted time: 10000[τ] par. one parameter.

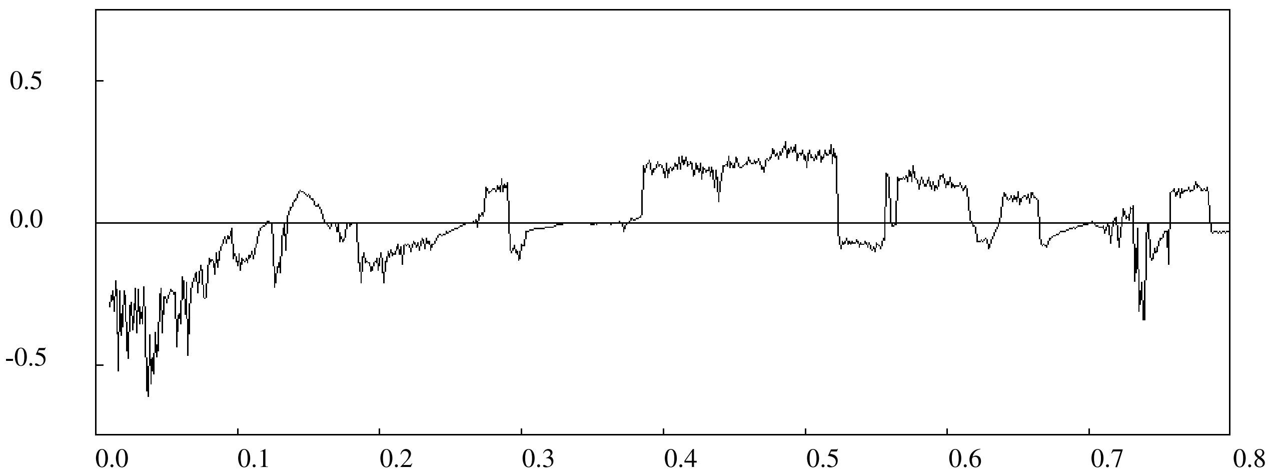

Figure 7: Largest Lyapunov exponent. Horizontal axis: α. $0.01 \leq \alpha \leq 0.80$. Parameter Step: 0.001.